LISBOA
UNIVERSIDADE DE LISBOA

FACULDADE DE MEDICINA LISBOA

TRABALHO FINAL
MESTRADO INTEGRADO EM MEDICINA

Instituto de Biologia Molecular

Expression profiles of *BRCA1/2* and homologous recombination genes in ovarian cancer

Maria Inês Fernandes Ribeiro

JUNHO'2021

LISBOA
UNIVERSIDADE DE LISBOA

FACULDADE DE MEDICINA LISBOA

TRABALHO FINAL
MESTRADO INTEGRADO EM MEDICINA

Instituto de Biologia Molecular

Expression profiles of *BRCA1/2* and homologous recombination genes in ovarian cancer

Maria Inês Fernandes Ribeiro

Orientado por:

Noélia Maria Fernandes Custódio

Co-Orientado por:

Rosina Savisaar

JUNHO'2021

Resumo

O cancro do ovário é uma das neoplasias ginecológicas mais letais e a mais difícil de tratar, possuindo uma elevada taxa de recidiva. Os inibidores de Poly (ADP-ribose) polymerases (PARPi) são uma das novas terapêuticas mais eficazes para o tratamento do cancro do ovário. Contudo, é crucial a existência de biomarcadores preditivos de maneira a clarificar a melhor estratégia para a utilização de PARPi. Os PARPi são letais especificamente para as células cancerígenas que não conseguem reparar o DNA através do mecanismo de recombinação homóloga (HR) e a deficiência da HR encontra-se frequentemente associada a mutações *BRCA1/2*. Os testes genéticos para *BRCA1/2* são atualmente utilizados na prática clínica, mas os resultados podem ser inconclusivos devido à elevada prevalência de variantes raras de significado indeterminado (VUS) na sequência do DNA. Adicionalmente, a maioria dos testes falha na deteção de modificações epigenéticas e de mutações localizadas em intrões que poderão alterar o mRNA. O objetivo deste trabalho foi investigar se a quantificação dos níveis de mRNA de *BRCA1/2* poderia fornecer informação além dos testes de DNA. Utilizando a tecnologia nCounter® da NanoString Technologies, analisamos RNA isolado de 38 amostras de cancro do ovário e de 11 amostras normais de trompas uterinas. Verificamos que a expressão de *BRCA1/2* foi muito variável entre tumores, tendo a maioria deles níveis de mRNA superiores ao tecido normal. Os nossos resultados também revelaram que os tumores com níveis mais elevados de mRNA de *BRCA1* ou *BRCA2* demonstraram uma sobrerregulação da expressão dos outros genes da HR. Estes resultados sugerem que medir os níveis de mRNAs de BRCA1/2 em tumores pode ajudar a prever quais pacientes obterão mais benefícios com a quimioterapia à base de platina e PARPi.

Palavras-chave: cancro do ovário; mRNA *BRCA1/2*; recombinação homóloga; tecnologia nCounter®

Abstract

Ovarian cancer is one of the most lethal gynecologic malignancies and the most difficult to treat, with a high rate of recurrence. Poly(ADP-ribose) polymerase inhibitors (PARPi) are one of the most effective new therapies for the treatment of ovarian cancer. However, for the greatest benefit of ovarian cancer patients, predictive biomarkers are essential to define the best strategy to use PARPi. Cancer cells that cannot repair DNA by homologous recombination (HR) are specifically sensitive to PARPi and HR deficiency is frequently associated with *BRCA1/2* mutations. Genetic tests for *BRCA1/2* are currently used in the clinic, but due to the high prevalence of rare DNA sequence variants of unknown significance (VUS), the results can frequently be inconclusive. In addition, most tests fail to detect epigenetic modifications and mutations located deep within introns that may alter the mRNA. The aim of the present study was to investigate whether the quantification of *BRCA1* and *BRCA2* mRNA levels in ovarian cancer could provide information beyond the DNA tests. We analyzed *BRCA1/BRCA2* mRNA expression using the nCounter® assay from NanoString Technologies, in RNA isolated from 38 ovarian cancer specimens and 11 normal fallopian tube samples. We found that *BRCA1/2* expression was highly variable among the analyzed tumors, with the majority having higher levels of mRNA compared to normal tissue. Our results further revealed that tumors with higher levels of *BRCA1* or *BRCA2* mRNA showed upregulated expression of 12 additional HR genes, while tumors with lower levels of *BRCA1/2* mRNA showed downregulated expression of HR genes. In summary, we show that *BRCA1/2* expression correlates with that of other HR genes. This suggests that measuring the levels of *BRCA1/2* mRNAs in tumors may help predicting which patients will gain the most benefit from platinum-based chemotherapy and PARPi.

Keywords: ovarian cancer; *BRCA1/2* mRNA; homologous recombination; nCounter® assay.

O Trabalho Final é da exclusiva responsabilidade do seu autor, não cabendo qualquer responsabilidade à FMUL pelos conteúdos nele apresentados.

Table of contents

Introduction

1. Ovarian cancer

Ovarian cancer is the eighth most common type of cancer and the eight-leading cause of death among female malignant diseases. In 2020, there were 313,959 new diagnosed cases and 207,252 deaths worldwide (Sung et al., 2021). Regarding gynecological malignancies, ovarian cancer is the second most common (after cervical cancer) and globally it is responsible for almost 5% of all female cancer death (Sung et al., 2021).

The 5-year relative survival rate for ovarian cancer is only 49%, which can be explained by the fact that most patients are diagnosed in advanced stages of the disease (American Cancer Society, 2021). This high fatality rate is related to the lack of specific early symptoms, the prevalence of aggressive high-grade serous carcinomas and the shortage of effective detection strategies (Torre et al., 2018).

About 90% of ovarian tumors are considered as having arisen from the transformation of epithelial cells in contrast to those derived from germ cells or sex-cord-stromal tissues (Matulonis et al., 2016). These are therefore designated as epithelial ovarian cancers (EOCs). EOCs comprise four well-defined histological subtypes: serous, mucinous, clear-cell and endometrioid – designations originated from their morphology and tissue architecture as observed through microscopy. The assignment of a tumor grade considering the degree of cytological aberration further stratifies serous and endometrioid EOCs. Hence, despite the similarities in histological appearance and terminology, high-grade and low-grade serous carcinomas of the ovary are regarded as being two distinct entities, with different sites of origin, types of carcinogenesis and molecular and genetic characteristics (Lisio et al., 2019).

2. DNA damage response (DDR) in the context of ovarian cancer treatment

High-grade serous ovarian cancer (HGSOC) is the most common type of EOC, being responsible for 75% of all EOCs (Lheureux et al., 2019). It also accounts for 70-80% of ovarian cancer deaths (Bowtell et al., 2015). Although the majority of HGSOCs are sporadic, approximately 15% to 20% of the cases are associated with germline

mutations in *BRCA1* (BReast CAncer gene 1) and *BRCA2* (BReast CAncer gene 2) genes, which are involved in repairing DNA lesions through the homologous recombination (HR) pathway (Alsop et al., 2012). Deleterious germline mutations in either *BRCA1* or *BRCA2* confer a high risk for breast and ovarian cancer, as well as a lesser increase in risk for other cancers (Metcalfe et al., 2010). From another perspective, around 44% of *BRCA1* mutation carriers will develop ovarian cancer by age 80, while this risk is 17% for *BRCA2* mutation carriers (Kuchenbaecker et al., 2017). The neoplasms occurring in these women usually manifest at an earlier age than in sporadic cases (Webb & Jordan, 2017). In addition to inherited mutations, somatic mutations in either of the *BRCA* genes are also found in HGSOCs (Lisio et al., 2019).

A feature of HGSOC is defective DNA-damage response (DDR), which comprises DNA repair and cell-cycle checkpoint pathways. In fact, current data suggests that all HGSOCs harbor a defect in at least one major DDR pathway. However, it must be underlined that defective DDR is not mediated through a single mechanism but rather from a myriad of genetic or epigenetic lesions affecting one or more of the five major DNA repair pathways – mismatch repair (MMR), base excision repair (BER), and nucleotide excision repair (NER) for single strand breaks (SSBs) and homologous recombination (HR) and non-homologous end joining (NHEJ) for double strand breaks (DSBs) (Gee et al., 2018).

DSBs repaired by HR are first end resected to generate 3' single-stranded DNA (ssDNA) that binds to the DNA recombinase RAD51 to form a nucleoprotein filament, which promotes strand invasion into a homologous duplex to initiate repair synthesis (Prakash et al., 2015). BRCA1 functions both in 5' to 3' resection of DSBs to generate 3' ssDNA overhangs, and in loading of RAD51 onto the ssDNA, whereas BRCA2 binds directly to RAD51 and localizes it to damaged DNA (Prakash et al., 2015). In the absence of functional BRCA1 or BRCA2, DSBs tend to be repaired by NHEJ in which the two broken DNA ends are joined without using a homologous DNA sequence to guide repair. Compared to HR repair, NHEJ is much more error-prone and often results in the introduction of DNA mutations, namely DNA deletions, which can affect the function of critical cancer genes thereby driving oncogenesis (Lord & Ashworth, 2012).

Since defects in DNA repair pathways are a key hallmark of ovarian cancer tumors, targeting DDR is nowadays one of the most extensively studied therapeutic approaches (Brown et al., 2017; Pilié et al., 2019).

2.1 Platinum-based chemotherapy

The standard treatment for HGSOC is maximal cytoreductive surgery, also known as “debulking surgery”, followed by platinum-based chemotherapy (Cortez et al., 2018). Although at least 70% of ovarian cancers will initially respond favorably to the first application of platinum-based chemotherapy (Bowtell et al., 2015), it is estimated that more than 80% of these will eventually relapse at some stage (Matulonis et al., 2016). The functional status of DNA repair, along with the remaining network of genes involved in the DDR, that is, the cell-cycle checkpoint pathways, influence the prognosis and the efficacy of chemotherapy (Lord & Ashworth, 2012; Pilié et al., 2019; Tomasova et al., 2020).

2.2 The role of poly(ADP-ribose) polymerase inhibitors (PARPi) in HGSOC

Over the last decade, the small molecule drugs that inhibit poly(ADP-ribose) polymerase (PARP) have been successfully implemented in recurrent HGSOC. PARP1 is the main target of PARP inhibitors (PARPi) and is primarily involved in the repair of SSBs. PARP1 binds to SSBs and ADP-ribosylates itself (autoPARylation) and other proteins, which recruits a series of repair enzymes that are essential for repairing the SSBs. Hence, the inhibition of PARP1 enzyme leads to the persistence of SSBs, that generate DSBs when a replication fork passes through during S phase. Normally, PARP1 inhibition alone is not lethal as the DNA lesions caused by these drugs can be repaired by other DNA repair pathways, specifically HR. However, in the absence of BRCA1/2 and therefore defective HR, the DNA lesions caused by PARPi are not repaired and cause cytotoxicity. This occurs due to the use of alternative error-prone DNA repair pathways that lead to a fragmentation of the genome of these cells and eventually results in their death (Mateo et al., 2019).This treatment is based on the concept of synthetic lethality, a phenomenon in which two genetic mutations are not lethal per se, but concomitant inactivation can result in cell death (Cortez et al., 2018).

Olaparib, the first approved PARPi, was originally targeted at HGSOC patients with germline mutations in the *BRCA1* or *BRCA2* genes. Nevertheless, its indications were later extended to all patients with recurrent HGSOC who were in a complete or partial response to platinum-based chemotherapy, regardless of the *BRCA1/2* status, even though responses were higher among the mutation carriers (Mateo et al., 2019). Concerning the non-carriers of *BRCA1/2* mutation, some had somatic *BRCA1/2* mutations and others had mutations in other genes of the HR pathway. These clinical trials were performed in patients previously treated with platinum-based chemotherapy, which causes DNA cross-links that are repaired in part by HR (Mateo et al., 2019). In fact, there is a clear association between the sensitivity to platinum-based chemotherapy, defined based on the time gap from last platinum exposure to disease progression, and the response to PARPi (Fong et al., 2010).

Predictive biomarkers for ovarian cancer therapy with PARPi are of utmost importance to define the best strategy for their use and, therefore, provide opportunities for targeted cancer therapy. Massively parallel sequencing technology enables detection of germline and somatic mutations in *BRCA1* and *BRCA2,* which has been used as predictive for the use of PARPi, however, the high prevalence of DNA variants of unknown significance (VUS) is a major limitation. Also, many of the genetic tests used in clinical practice do not detect epigenetic modifications and mutations located deep within introns that may alter the pre-mRNA processing (Vaz-Drago et al., 2017).

Motivation and Aims of the Project

The main goal of this project is to establish proof-of-principle that measuring the level of *BRCA1/2* mRNA in ovarian cancer tissue may be useful to uncover BRCA1/2 deficiencies that could be used to predict response to PARPi when DNA tests are negative or inconclusive. Since response to PARPi has also been attributed to mutation in other genes related to DNA damage and repair pathways, another aim was to analyze the expression of additional genes of these pathways. To achieve this goal, a novel screening approach was applied, making use of the cutting-edge NanoString technology, which provides sensitive and precise absolute quantification of mRNA molecules in biological samples, including archived formalin-fixed and paraffin-embedded (FFPE) tissues (Reis et al., 2011).

We think that measuring the level of *BRCA1/2* mRNA in ovarian cancer tissue may be useful because lower levels of *BRCA1/2* mRNA have been shown to cause dysfunctional expression of BRCA1/2 proteins, resulting in HR deficiency and sensitivity to PARPi (Peng et al., 2014). Therefore, our expectation was that by measuring the level of *BRCA1/2* mRNA we could uncover *BRCA*-deficient ovarian cancers missed by the conventional DNA-based methods and thereby predict the sensitivity to PARPi. Indeed, epigenetic silencing and frameshift mutations can lead to reduced mRNA levels. Concerning the frameshift mutations, besides the classical indels (insertions or deletions) of nucleotides, splicing mutations may also produce a frameshift due to exon skipping, alternative splicing or intron retention (Vaz-Drago et al., 2017). The mRNA molecules may then be degraded by nonsense-mediated mRNA decay (NMD) because the frameshift mutation may introduce a premature termination codon (PTC) (Chang et al., 2007). As a result, there is a downregulation of the mRNA, resulting in loss-of-function of the affected genes, which may predispose to cancer, specifically when it affects tumor suppressor genes (Hu et al., 2017).

My contribution to this work was extracting the RNA from the ovarian tumor samples and the normal samples, evaluating its quantity and quality in the Agilent 4200 TapeStation System and then analyzing the data of the Nanostring nCounter® Analysis System with the nSolver software. All these procedures were made with the help and

under the guidance of my supervisor Professor Noélia Custódio. Doctor Rosina Savisaar, my co-supervisor, performed the statistical analysis of the results.

Materials and Methods

Biological samples

Archived FFPE tissue biopsies, including ovarian cancer and normal fallopian tube samples, were analyzed. Samples were collected from the archives of Hospital Santa Maria/Centro Hospitalar Universitário Lisboa Norte, Lisbon, Portugal and Instituto Português de Oncologia, Porto, Portugal. The study was approved by the ethical committee of the Lisbon Academic Medical Center, Lisbon, Portugal (approval number: 170/18). The quality of each sample was assessed by an experienced pathologist. In the case of tumor samples, the diagnosis was confirmed, and the tissue was macrodissected to ensure that only tumor regions were analyzed.

RNA isolation and quantification

For RNA extraction from FFPE samples, 8 curls of tissue (10µm thick) were used for larger tumor areas and 20 curls of tissue (14µm thick) were used for small tumor areas. Prior to RNA extraction, one tissue section was taken from each sample, stained with hematoxylin and eosin (H&E) and examined by a pathologist to localize tumor cells (**Figure 1**).

Figure 1: Sectioning of an ovarian tumor sample from an FFPE tissue block. In this case (sample 6), only part of the area of the sample was tumor. This area was first marked in the paraffin and then recovered from the microtome slices (20 slices/14µm). For larger tumor areas 8 slices of 10µm were used.

RNA was purified using the PureLink™ FFPE RNA Isolation Kit (ThermoFisher Scientific) (Patel et al., 2017). Subsequently, the amount and purity of the total RNA recovered was determined with the Nanodrop™ 2000 spectrophotometer. The A260/280 ratio was used to determine protein contamination as aromatic proteins have a strong UV absorbance at 280 nm. For pure RNA, A260/280 ratios should be ~1.8 and a lower ratio indicates likely protein contamination. The results indicated that all samples

were free of protein contamination. The A260/230 ratio indicates the presence of organic contaminants. In a pure sample, the A260/230 should be close to 2.0. Some of the samples had A260/230 ratios below 1.8, which indicated organic contaminants, but these samples were still acceptable to use in NanoString nCounter® gene expression assays. The final step of the purification of the RNA samples is the degradation of traces of contaminant DNA using DNase I digestion. Following this treatment, the precise RNA concentration and degree of fragmentation was analysed in the Agilent 4200 TapeStation system using the Agilent RNA ScreenTape assay. For NanoString nCounter® gene expression assays, it is recommended that at least 50% of the sample be greater than 300 nucleotides (nt) in length for optimal performance.

Gene expression profiling with the nCounter® system

For gene expression profiling, the nCounter® FLEX Analysis System was used with the Vantage 3D™ RNA Panel for DNA Damage and Repair (NanoString Technologies, Seattle, WA, USA). The mRNA hybridization, detection and scanning were performed at the Nanostring nCounter® Core Facility at Serviço de Genética - Instituto Português de Oncologia do Porto Francisco Gentil, E.P.E., Porto, Portugal. An overview of the procedure for quantification of gene expression in the Nanostring nCounter® Analysis System is shown in **Figure 2.** Briefly, purified RNA (200ng) was hybridized overnight at 67 ℃. The full volume of the hybridization reactions was immediately introduced in the Prep Station, which is a liquid handling robot that performs the purification of the hybridized complexes and their immobilization onto the surface of a cartridge. The barcodes captured for each sample were then identified and counted by the Digital Analyzer. The resulting data was imported into and analyzed by the nSolver 4.0 Analysis Software System. Quality control parameters recommended by NanoString were applied using the nSolver default settings. Samples that failed the quality control metrics were excluded from further analysis. For data normalization, raw counts were first background adjusted using the internal negative controls followed by a within-sample normalization using the internal positive controls. Finally, data were normalized across samples (i.e., corrected for input) using the mean RNA counts from reference

(housekeeping) genes. This resulted in a total of 49 samples, 11 from normal fallopian tube and 38 from ovarian cancer tissue.

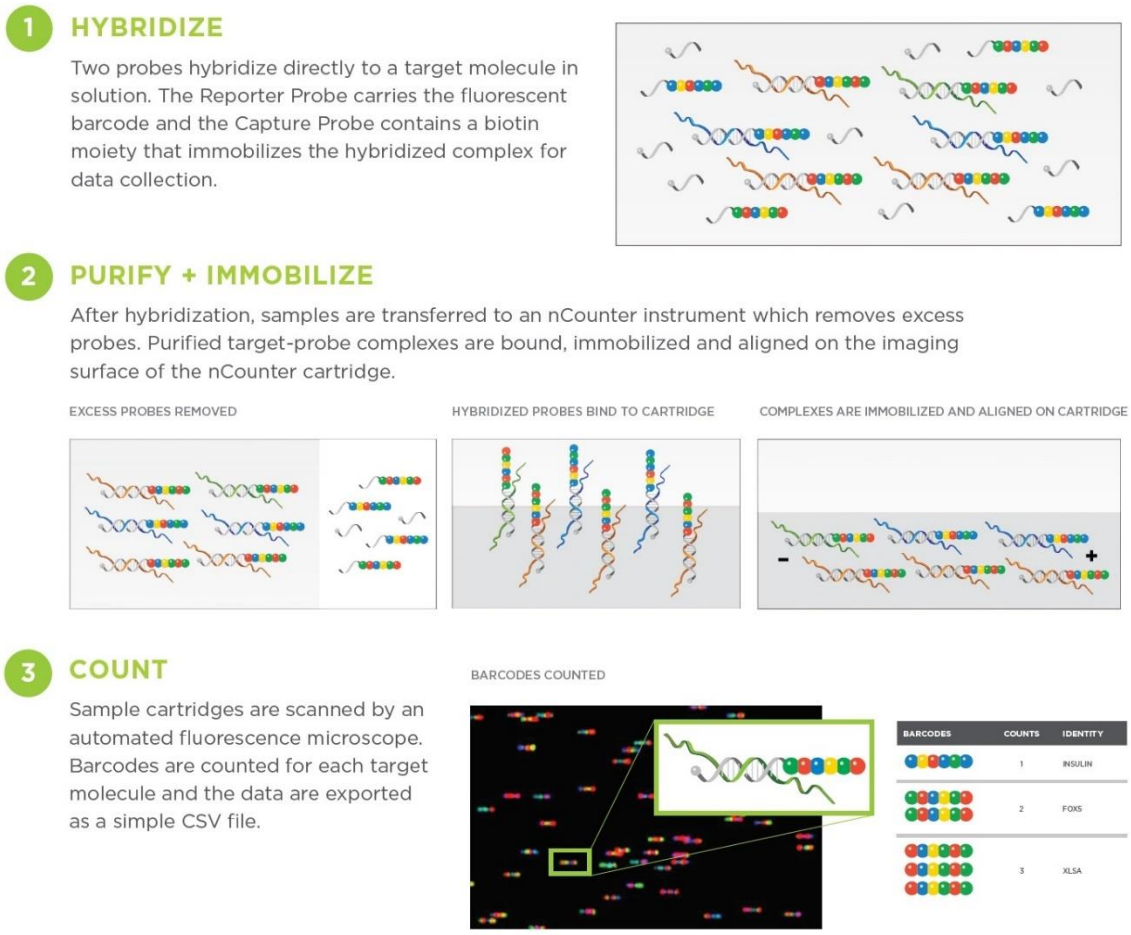

Figure 2: Schematic representation of the main steps of nCounter® Analysis System (https://www.nanostring.com).

Statistical analysis

General

Analysis and plotting were performed with R version 3.6.1 (R Core Team 2019). Empirical *P*-values were calculated as as $P = \frac{n+1}{m+1}$, where n is the number of simulants that show a value as high as or higher than the true value, and m is the total number of simulants (North et al., 2003). Spearman's correlation coefficients were converted to z'-values and back using the functions *FisherZ()* and *FisherZInv()* in the DescTools package v. 0.99.36.

Analysis of NanoString data

Genes were classified into pathways based on the labels supplied with the NanoString panel used. The Homologous Recombination and Fanconi Anemia pathways were grouped together, and the relevant genes will be referred to as Homologous Recombination (HR) genes through-out the text. Twelve of the genes in the panel (*ERCC1*, *ERCC2*, *ERCC3*, *ERCC4*, *ERCC5*, *ERCC6*, *ERCC8*, *EXO1*, *FAN1*, *FANCA*, *FANCB*, *FANCC*) were excluded from the analysis because of quality control issues with their probes in one of the runs. Note that a few of the samples were included in two separate NanoString runs. In these cases, the values from the two runs were averaged after data normalization in the nSolver software. The heatmap in **Figure 6** was produced with the *heatmap.2* function from the *gplots* package version 3.0.1.1 (Warnes et al. 2019), using the complete linkage clustering method with $1 - Spearman's\ \rho$ as the distance function. Prior to generating the heatmap, data was scaled so that the mean of each gene was 0 and the standard deviation was 1 to normalize for differences in NanoString probe efficiency.

Results

Cohort of the study

The cohort of this study consists of 42 FFPE tissue samples from patients diagnosed with ovarian cancer, the majority of which were classified as HGSOC (**Supplementary Table 1**). All tumor tissues were previously screened for the presence of mutations in the *BRCA1* and *BRCA2* genes using conventional DNA-based methods and the results are indicated in **Supplementary Table 1**. These tumor samples include samples that carry established pathogenic *BRCA* mutations, new variants of unknown significance, as well as samples lacking any known *BRCA* mutation. Because it has been established that the majority of HGSOC derive from epithelium of the fallopian tube (Hu et al., 2020; Labidi-Galy et al., 2017; Lisio et al., 2019), 18 samples of normal fallopian tubes surgically resected from individuals with no cancer diagnosis were included as controls in the study (**Supplementary Table 2**).

BRCA1 and *BRCA2* mRNA-expression is correlated with the expression of other HR genes

To measure transcripts levels in RNA extracted from FFPE tissue samples, we used the cutting-edge nCounter® assay from NanoString Technologies. This technology has been shown to provide sensitive and precise absolute quantification of mRNA molecules in biological samples, including low-quality RNA samples such as archived FFPE tissues (Reis et al., 2011). The NanoString nCounter® system is an automated system that provides a direct measurement of gene expression using a digital color-coded barcode technology. This works by directly capturing, imaging, and counting fluorescent barcodes hybridized to individual nucleic acid molecules, without requiring the conversion of mRNA to cDNA by reverse transcription or the amplification of the resulting cDNA by PCR. In fact, comparing to real-time PCR, it has been shown to have similar sensitivity, but with the advantage of avoiding the bias introduced by the reverse transcription of mRNA and subsequent cDNA amplification (Geiss et al., 2008).

Analysis of the RNA integrity number (RIN) of extracted RNA from the FFPE samples indicated it was degraded and the mean RIN was 2.4 (range 1.8-5.0); this result was expected since formalin fixation is known to affect the quality of the RNA extracted from FFPE archival tissues. RNA concentrations ranged from 19.7 to 353.4 ng/µL (**Figure 3A**, **Supplementary Table 1** and **Supplementary Table 2**). It is recommended by NanoString Technologies that at least 50% of the sample is greater than 300 nucleotides in length for optimal performance (**Figure 3B**). Consequently, the samples that did not meet this criterion were discarded from further analysis. Also, quality control parameters recommended by NanoString were applied using the nSolver default settings and samples that failed the quality control metrics were excluded from further analysis (**Figure 4**).

A

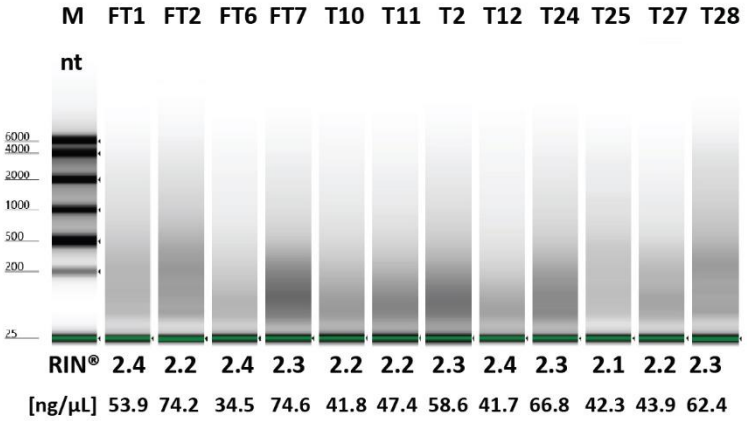

B

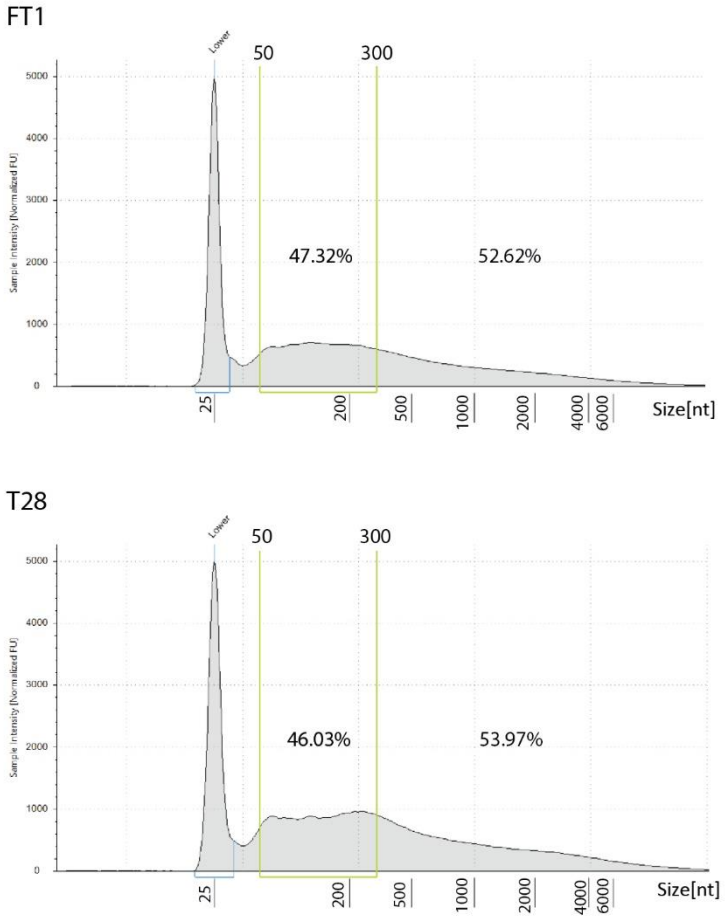

Figure 3: FFPE Samples for NanoString analysis. **(A)** Evaluation of RNA quantity and quality with the 4200 TapeStation (Agilent Technologies, Santa Clara, CA) using the Agilent RNA ScreenTape Assay. Concentration (ng/µL) and RIN (RNA integrity number) values for a representative group of control and tumor samples is shown. **(B)** Representative electropherograms of RNA retrieved from fallopian tube sample FT1 and ovarian tumor sample T28. The percent of samples greater than 300 nt was estimated by the percent of the sample between 50–300nt and subtracting that quantity from 100%.

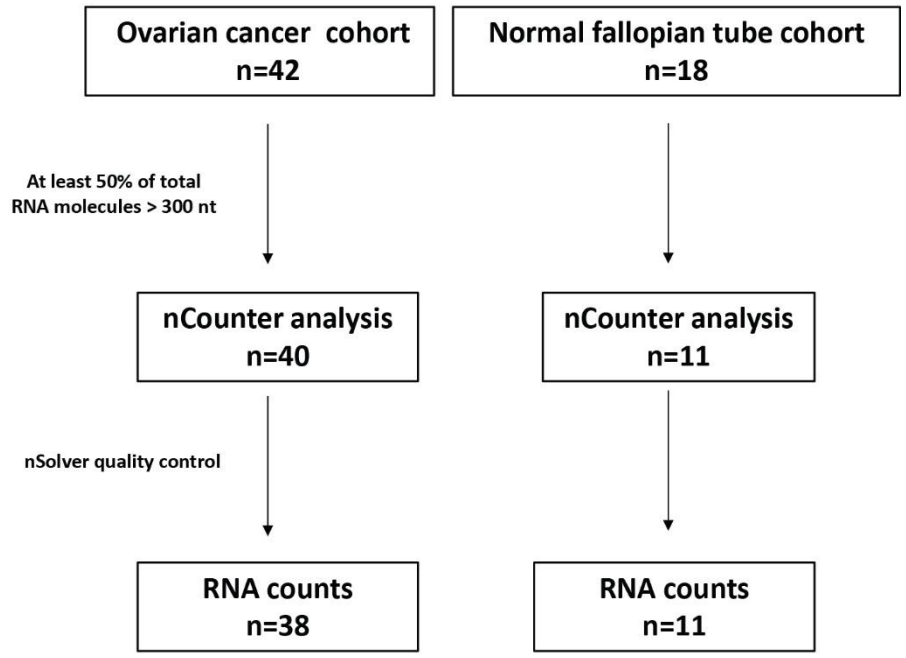

Figure 4: Overview of FFPE samples used in the study.

In this study we used the nCounter® Vantage™ RNA Panel for DNA Damage and Repair, which is composed of a total of 192 genes, with 12 housekeeping genes and 180 unique genes related to DNA damage and repair pathways, including *BRCA1* and *BRCA2* (**Supplementary Table 3**).

When analyzing the expression of *BRCA1* and *BRCA2* genes in the different samples of normal fallopian tubes the results showed little variation (**Figure 5A**). In contrast the levels of *BRCA1* and *BRCA2* mRNA was highly variable among the tumors, with some samples showing levels lower than the control samples and others having levels that were almost 10-fold higher than the median of normal samples (**Figure 5A**). The results also showed a significantly higher median mRNA expression for tumors compared to normal fallopian tubes, both for *BRCA1* (normal median: 195.23; tumor median: 256.52; $p \sim 0.010$, two-tailed Mann-Whitney *U*-test) and *BRCA2* (fallopian tube median: 74.13; tumor median: 305.87; $p \sim 5.59 * 10^{-12}$, two-tailed Mann-Whitney *U*-test).

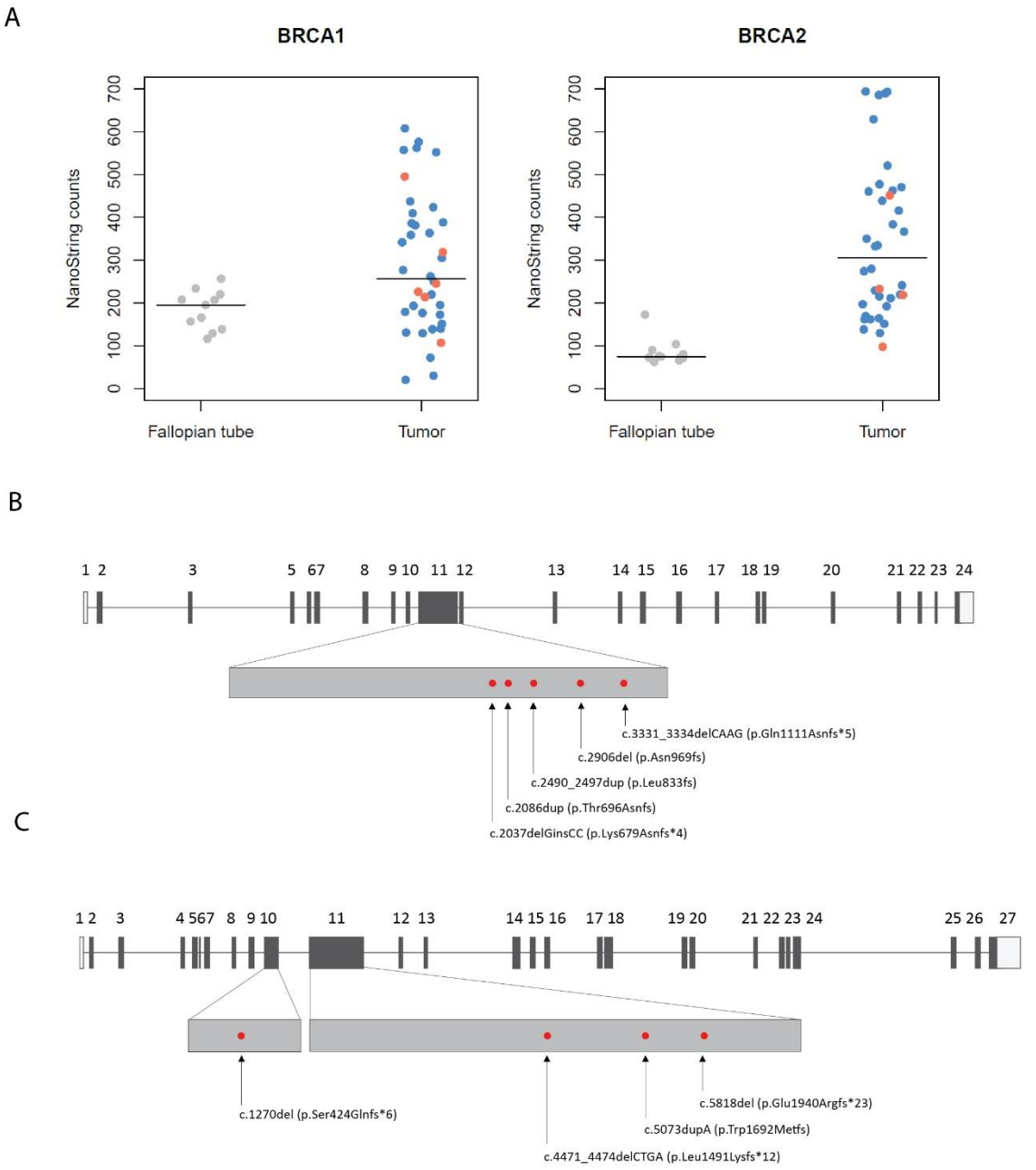

Figure 5: (A) Expression level of BRCA1 and BRCA2 genes in 11 normal fallopian tube and 38 tumor samples analyzed with the NanoString nCounter assay. Red dots denote tumors with frameshift mutations; blue dots denote all other tumors. The horizontal line represents the median counts for the normal fallopian tube samples and the tumor samples, respectively. **(B)** Schematic representation of BRCA1 gene. BRCA1 exons are numbered 1 to 24. Frameshift mutations in exon 11 that generate PTC s are indicated. **(C)** Schematic representation of BRCA2 gene. BRCA2 exons are numbered 1 to 27. Frameshift mutations in exon 10 and exon 11 that generate PTCs are indicated.

Focusing then on tumors with frameshift mutations that generate PTCs, we confirmed that all the frameshift mutations are predicted to elicit NMD according to validated rules (Lindeboom et al., 2016). They all are more than 200 bp downstream of the start codon and more than 50-54 bp upstream of the last exon-exon (**Figure 5B** and **C**). Despite big variability in *BRCA1/2* mRNA levels observed among tumors, those with

frameshift mutations were amongst the ones with lower levels of *BRCA1* or *BRCA2* expression (**Figure 5A**). Five tumors had frameshift mutations located in *BRCA1* exon 11 (**Figure 5B**) and four tumors had frameshift mutations located in *BRCA2* exons 10 and 11 (**Figure 5C**). In these samples, the median *BRCA1* expression was 235.63 (median of all tumors: 256.52), and the median *BRCA2* expression was 225.71 (median of all tumors: 305.87). In addition, four of the analyzed tumors had missense mutations. In tumors with *BRCA1* missense mutations the median *BRCA1* expression was 409.64, whereas in the tumor with a *BRCA2* missense expression of *BRCA2* was 477.36. Three tumors had the c.156_157insAlu *BRCA2* mutation, which has only been reported in families of Portuguese ancestry and represents 55% of all *BRCA2* germinal mutation carriers in Portugal (Peixoto et al., 2015). This mutation leads to full in-frame skipping of exon 3 (Machado et al., 2007; Peixoto et al., 2015), and the median *BRCA2* expression was 438.28.

Next, the expression of additional genes related to DNA damage and repair was analyzed. There were strikingly different expression patterns between normal and tumor samples (**Figure 6**) with 72 genes significantly differentially expressed (two-tailed Welch's t-test on ranks with Bonferroni correction; genes were significantly differentially expressed if the corrected P-value was below 0.05; **Table 1**).

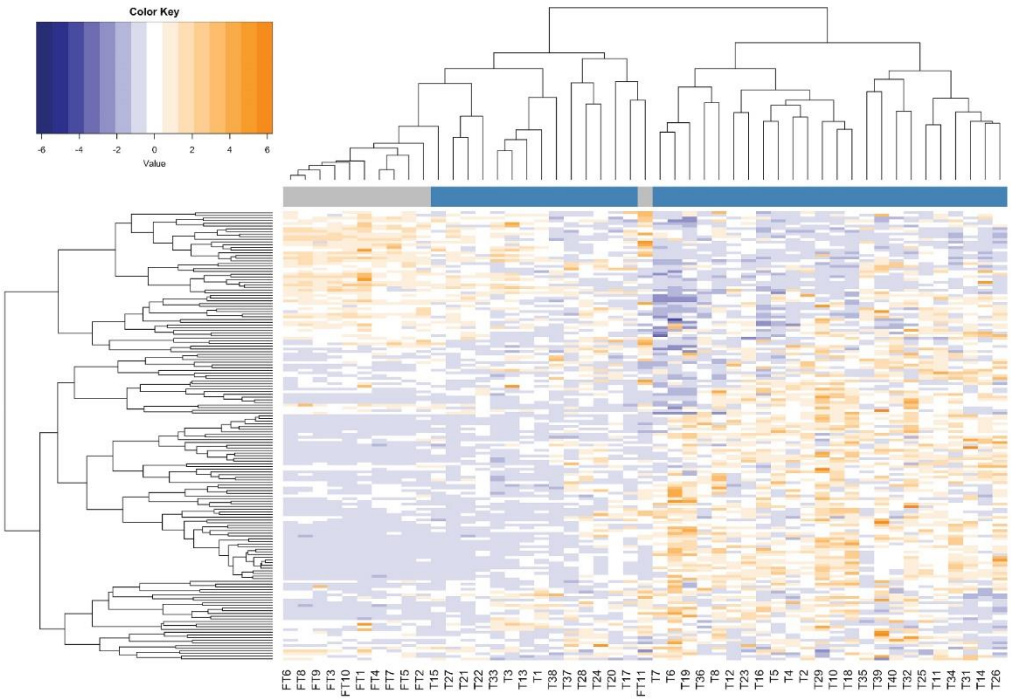

Figure 6: Heatmap for mRNA counts obtained with the NanoString nCounter assay for DNA damage and repair genes in 11 normal fallopian tube and 38 tumor samples. Genes are depicted in rows and samples in columns. Both rows and columns have been clustered based on Spearman correlations. Normal fallopian tube (FT) samples are labelled in grey, whereas tumour samples (T) are labelled in blue. Note that the data has been scaled and centred in rows, so that the row mean is 0 and the row standard deviation is 1.

Table 1: Genes significantly differentially expressed in tumors.

A) Genes upregulated in tumors

Pathway	Genes
Apoptosis	*BCL2L1*, CASP8, *MYD88*
Base excision repair	*APEX2, FEN1, NEIL3, PARP1, SMUG1, UNG*
Base excision repair - Translesion Synthesis - Cell Cycle and Signaling	*PCNA*
Cell Cycle and Signaling	*AURKA*, *BUB1B*, *CDKN2A, KRAS, RAD21, RM12, SUMO3*
Checkpoint Activation	*H2AFX*
Checkpoint Activation - Cell Cycle and Signaling	*CHEK1/2*
Homologous Recombination and Fanconi Anemia	*BRIP1, BLM, BRCA2, FANCD2, FANCG, FANCI, GEN1, RAD51*, *RAD54L, UBE2T, USP1, XRCC2,* XRCC3
Independent Repair Enzymes/Polymerases	*DNA2*, *POLQ*
Independent Repair Enzymes/Polymerases-Base excision repair	*POLD1*, *POLD4*, *POLE2*
Independent Repair Enzymes/Polymerases - Cell Cycle and Signaling	*MAD2L2*
Independent Repair Enzymes/Polymerases-	*POLR2D, POLR2H*

Nucleotide Excision Repair	
Independent Repair Enzymes/Polymerases-Translesion Synthesis	*HLTF*
Mismatch Repair	*MSH2*
Mismatch Repair- Translesion Synthesis	*RFC4*
Non-homologous End joining - Cell Cycle and Signaling	P*RKDC*
Translesion Synthesis	*RAD18*
Housekeeping	SF3FA3

B) Genes downregulated in tumors

Pathway	Genes
Apoptosis	*AKT3, BCL2, NFKB2, PIK3R1*
Base Excision Repair	*NEIL1, NEIL2, OGG1*
Cell Cycle and Signaling	*ABL1, CCND2, CDKN1A, EGFR*
Checkpoint Activation	*TIPIN*
Homologous Recombination and Fanconi Anemia	*RAD51B, WRN*
Independent Repair Enzymes/Polymerases	*ALKBH3, CRY1, POLK, REV1*
Independent Repair Enzymes/Polymerases - Translesion Synthesis	*POLI*
Mismatch Repair	*MSH3*
Non-homologous End joining	*LIG4*
Nucleotide Excision Repair	*XPA*
Nucleotide Excision Repair - Apoptosis	*PTEN*
Housekeeping	*COG7, NUBP1*

Among the 47 genes showing higher expression in tumors, 13 (~28%) belonged to the HR and Fanconi Anemia pathway (**Table 1A**, **Supplementary Figure 1 A-C**). Only two genes in this pathway were significantly downregulated in tumors (**Table 1A**, **Supplementary Figure 1D** and **E**). This observation suggested that the expression of genes that belong to the HR pathway might be coordinately regulated. To explore this, the cohort was then divided into low and high groups based on the *BRCA1/2* mRNA counts due to the heterogeneity of *BRCA1/2* expression among the tumor samples. The low group includes tumors with *BRCA1/2* mRNA levels equal to or below the median value observed in tumors with frameshift mutations, while the high group includes tumors with mRNA levels above that threshold value. **Figure 7A** and **B** shows that the

expression of significantly differentially expressed HR genes is systematically downregulated in the *BRCA1/2* low groups and upregulated in the *BRCA1/2* high groups.

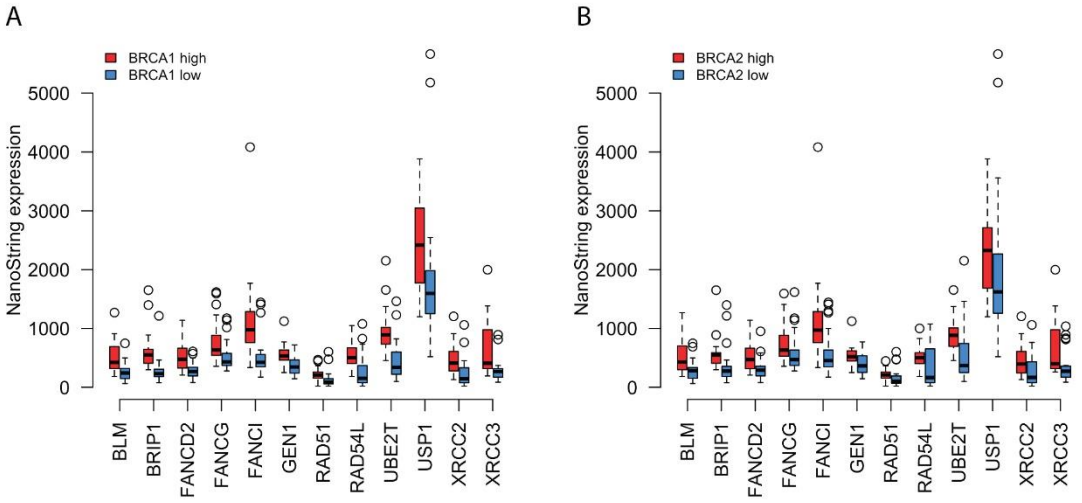

Figure 7: Coordinated expression of BRCA1/2 and HR genes that were found upregulated in tumors compared to normal tissue. **(A-B)** NanoString expression values for the identified HR genes when BRCA1/2 expression is above or below the median for tumors with frameshift mutations.

Discussion and Conclusions

In this work, we compared levels of *BRCA1* and *BRCA2* mRNA between ovarian tumors, most of them HGSOC, and normal fallopian tubes, the place of origin of these neoplasms (Hu et al., 2020; Labidi-Galy et al., 2017; Lisio et al., 2019). To accomplish this, we employed the cutting-edge NanoString nCounter® Technology, which allows the direct measurement of the number of RNA transcripts in biological samples, including archival FFPE tissue samples which contain highly fragmented RNA molecules.

The results indicate that *BRCA1* and *BRCA2* mRNA expression levels for the different tumors analyzed is highly heterogeneous. The results also show that the average expression levels of *BRCA1* and *BRCA2* in the tumors was higher than in the normal fallopian tube tissues. The higher levels of *BRCA1* and *BRCA2* mRNA in tumors may be explained by the fact that cancer cells proliferate rapidly, which in conjunction with genetic instability may increase the need for more DDR (Rajan et al., 1997; Tsibulak et al., 2018). In agreement with this, we found several cell-cycle related genes that were significantly upregulated in tumors (**Table 1A**).

All tumors exhibited levels of *BRCA2* expression similar to or higher than the median of normal tissues (**Figure 5A**). In contrast, several tumors expressed *BRCA1* at levels lower than the median of normal fallopian tube tissue (**Figure 5A**). Regarding these, some potential explanations can be provided. Firstly, epigenetic silencing because of promoter hypermethylation can lead to this reduction, which has been reported in the *BRCA1* gene in more than 10% of ovarian cancers (Baldwin et al., 2000; Esteller et al., 2000; Network, 2011). Secondly, microRNA-mediated regulation is another mechanism that can explain this phenomenon (Moskwa et al., 2011). Finally, the presence of frameshift mutations that can introduce a PTC and trigger mRNA degradation by NMD is also a possibility (Chang et al., 2007). In this study, among the tumors that showed lower levels of *BRCA1* and *BRCA2* expression than the median for normal samples, there were 9 tumors with frameshift mutations in these genes that were predicted to activate NMD.

Several reported studies suggest that a reduction in the expression of *BRCA1* and *BRCA2* in tumors results in defective DNA repair by homologous recombination. In one of these studies, it was shown that miR-182-mediated down-regulation of *BRCA1* impacts DNA repair by HR and sensitivity to PARPi (Moskwa et al., 2011). In addition, knockdown or *BRCA1 or BRCA2* in the MCF 10A cell line (a non-tumorigenic mammary epithelial cell line) causes a downregulation of mRNAs encoding other HR genes generating a HR deficiency (HRD) gene signature (Peng et al., 2014). Additionally, it has been reported that primary *BRCA1*-mutated tumors with recurrent resistance to platinum compounds exhibit secondary genetic changes within the *BRCA1* gene, which is accompanied by restored expression of BRCA1 protein (Swisher et al., 2008).

Our results also suggest that *BRCA1/2* expression is correlated with the expression of 12 additional HR genes, although this result is only significant for *BRCA2*. This may be explained by the fact that the role of BRCA2 in the DDR by HR is more direct and selective. Indeed, BRCA1 is also engaged in other cellular processes, like transcriptional regulation, cell cycle control and apoptosis, while BRCA2 is almost exclusively involved in HR by recruiting RAD51C to DSB sites (Tsibulak et al., 2020). For this reason, *BRCA2* may be a better surrogate marker for HR deficiency in HGSOC.

It is well established that the 'BRCAness' phenotype, which is applied to tumors with an HR defect but without detectable germline mutation in *BRCA1* or *BRCA2* genes, correlates with better responses to chemotherapy based on platinum salts and PARPi (Tsibulak et al., 2020). Our results support the idea that assessing levels of *BRCA1* and *BRCA2* in tumor samples may enable the assessment of the tumor HR status and therefore could help to predict which patients will respond more favorably to platinum-based chemotherapy and PARPi. This is particularly important when conventional BRCA DNA tests are negative or inconclusive. In agreement with this, there are several reports in the literature that describe an association between reduced *BRCA1* mRNA or BRCA1 protein levels in different types of cancer and response to cisplatin therapy (Carser et al., 2011; Gao et al., 2013; Huang et al., 2016; Quinn et al., 2007; Rosell et al., 2009; Taron et al., 2004; Wang et al., 2008).

Future validation studies in large cohorts are needed to determine whether *BRCA1* and *BRCA2* mRNA levels below or above a certain cut-off value can discriminate

between HR-deficient and HR-proficient tumors. This is of vital importance to the application of precision medicine.

Funding

This work was supported by grants from Programa “Educação pela Ciência” (project nr 20180024) from GAPIC/FMUL, Fundação para a Ciência e a Tecnologia (FCT), Portugal (PTDC/MED-ONC/29469/2017) and AstraZeneca HealthCare Foundation.

Supplementary Material

Supplementary Table 1: Tumor samples information.

Sample ID	Diagnosis	BRCA variant (Clinical significance-ClinVar)	RIN	Conc. [ng/µL]
T1	High-grade serous ovarian carcinoma	NM_007294.3(BRCA1):c.788G>T (p.Gly263val); exon 11 of ***BRCA1*** (Uncertain significance)	2.6	55.5
T2	High-grade serous ovarian carcinoma	NM_007294.3(BRCA1): c.5095C>T (p.Arg1699Trp); exon 18 of ***BRCA1*** (Pathogenic)	2.3	58.6
T3	High-grade serous ovarian carcinoma	NM_007294.3(BRCA1):c.3331_3334delCAAG (p.Gln1111Asnfs*5); exon 11 of ***BRCA1*** (Pathogenic)	1.9	87.1
T4	High-grade serous ovarian carcinoma	NM_007294.3(BRCA1):c.2037delGinsCC (p.Lys679Asnfs*4); exon11 of ***BRCA1*** (Pathogenic)	2.1	70.9
T5	High-grade serous ovarian carcinoma	NM_007294.3(BRCA1):c.3331_3334delCAAG (p.Gln1111fs); exon11 of ***BRCA1*** (Pathogenic)	–	173.5
T6	Papillary serous carcinoma poorly differentiated	NM_007294.3(BRCA1):c.2490_2497dup (p.Leu833fs); exon11 of ***BRCA1*** (Pathogenic)	–	93.2
T7	Ovarian Clear Cell Adenocarcinomas	NM_007294.3(BRCA1):c.2086dup (p.Thr696Asnfs); exon11 of ***BRCA1*** (Pathogenic)	–	29.6
T8	Poorly differentiated ovarian serous papillary carcinoma	NM_007294.3(BRCA1):c.2906del (p.Asn969fs);exon11 of ***BRCA1*** (Pathogenic)	–	353.4
T9	Mixed ovarian epithelial carcinoma with clear cell and serous components	NM_007294.3(BRCA1):c.3331_3334delCAAG (p.Gln1111fs); exon11 of ***BRCA1*** (Pathogenic)	–	102.2
T10	High-grade serous ovarian carcinoma	NM_007294.3(BRCA1):c.5453A>G, (p.Asp1818Gly); exon23 of ***BRCA1*** (Likely pathogenic)	2.1	106.0
T11	High-grade serous ovarian carcinoma	NM_000059.3(BRCA2):c.516+8T>C; intron 6 of ***BRCA2*** (New)	2.2	41.8

T12	High-grade serous ovarian carcinoma	NM_000059.3(BRCA2):c.4471_4474delCTGA (p.Leu1491Lysfs*12); exon 11 of ***BRCA2*** (Pathogenic)	2.2	47.4
T13	High-grade serous ovarian carcinoma	NM_000059.3(BRCA2):c.5818del (p.Glu1940Argfs*23); exon 11 of ***BRCA2*** (New)	2.4	41.7
T14	High-grade serous ovarian carcinoma	NM_000059.3(BRCA2):c.9986A>G (p.Asn3329Ser); exon 27 of ***BRCA2*** (Uncertain significance)	1.8	157.0
T15	Seromucinous ovarian carcinoma	NM_000059.3(BRCA2):c.1270del (p.Ser424Glnfs*6); exon 10 of ***BRCA2*** (New)	1.9	152.0
T16	High-grade serous ovarian carcinoma	NM_000059.3(BRCA2):c.5073dupA (p.Trp1692Metfs); exon11 of ***BRCA2*** (Pathogenic)	–	91.3
T17	Papillary serous carcinoma moderatly differentiated	NM_000059.3(BRCA2):c.156_157insAlu; exon3 of ***BRCA2*** (Pathogenic)	–	91.1
T18	Poorly-differentiated solid ovarian carcinoma with clear cell areas	NM_000059.3(BRCA2):c.156_157insAlu; exon3 of ***BRCA2*** (Pathogenic)	–	276.1
T19	Poorly-differentiated endometrioid ovarian adenocarcinoma	NM_000059.3(BRCA2):c.156_157insAlu; exon3 of ***BRCA2*** (Pathogenic)	–	133.4
T20	Ovarian endometrioid adenocarcinoma	negative	2.0	95.6
T21	High-grade serous ovarian carcinoma	negative	2.0	175.0
T22	High-grade serous ovarian carcinoma	negative	2.0	120.0
T23	Serous carcinoma of the right fallopian tube	negative	2.0	155.0
T24	High-grade serous ovarian carcinoma	negative	2.2	147.0
T25	High-grade serous ovarian carcinoma	negative	2.3	66.8

T26	Transitional cell carcinoma of the ovary	negative	2.1	42.3
T27	Serous ovarian carcinoma	negative	2.0	109.0
T28	Undifferentiated carcinoma of the ovary	negative	2.2	43.9
T29	Endometrioid carcinoma of the ovary	negative	2.3	62.4
T30	High-grade serous ovarian carcinoma	negative	2.3	71.9
T31	High-grade serous ovarian carcinoma	negative	1.8	114.0
T32	High-grade serous ovarian carcinoma	negative	1.9	139.0
T33	High-grade serous ovarian carcinoma	negative	2.3	112.0
T34	High-grade serous ovarian carcinoma	negative	5.0	68.3
T35	Low-grade serous ovarian carcinoma in borderline tumor	negative	3.3	197.0
T36	High-grade serous ovarian carcinoma	negative	2.2	174.0
T37	High-grade serous ovarian carcinoma	negative	2.3	180.0
T38	High-grade serous ovarian carcinoma	negative	2.1	60.4
T39	High-grade serous ovarian carcinoma	negative	4.2	144.0
T40	High-grade serous ovarian carcinoma	negative	2.7	194.0

T41	High-grade serous ovarian carcinoma	negative	2.1	28.8
T42	Low-grade serous ovarian carcinoma	negative	2.9	24.4

Supplementary Table 2: Fallopian tubes samples information.

Sample ID	**RIN**	**Conc. [ng/µL]**
FT1	2.4	53.9
FT2	2.2	74.2
FT3	2.2	52.8
FT4	2.2	61.5
FT5	3.4	52.4
FT6	2.4	34.5
FT7	2.3	74.6
FT8	2.4	45.7
FT9	2.2	48.9
FT10	3.3	77.6
FT11	2.4	125.0
FT12	2.2	26.8
FT13	3.0	19.7
FT14	2.5	31.4
FT15	2.7	45.1
FT16	3.0	48.1
FT17	2.2	58.7
FT18	1.9	91.2

Supplementary Table 3: List of genes in nCounter Vantage™ RNA Panel for DNA Damage and Repair and signature descriptions. This panel includes 192 genes, 180 unique genes related to DNA damage and repair pathways and 12 housekeeping genes for data normalization.

Official Symbol	Accession	Official Full Name	Pathways
ABL1	NM_005157.3	c-abl oncogene 1, non-receptor tyrosine kinase	Cell Cycle and Signaling
AKT3	NM_005465.4	v-akt murine thymoma viral oncogene homolog 3	Apoptosis
ALKBH2	NM_001001655.2	alkB, alkylation repair homolog 2 (E. coli)	Independent Repair Enzymes/Polymerases
ALKBH3	NM_139178.3	alkB, alkylation repair homolog 3 (E. coli)	Independent Repair Enzymes/Polymerases
APC	NM_000038.3	adenomatous polyposis coli	Cell Cycle and Signaling
APEX1	NM_001641.2	APEX nuclease (multifunctional DNA repair enzyme) 1	Base Excision Repair
APEX2	NM_014481.2	APEX nuclease (apurinic/apyrimidinic endonuclease) 2	Base Excision Repair
ATM	NM_138292.3	ataxia telangiectasia mutated	Checkpoint Activation - Apoptosis - Cell Cycle and Signaling
ATR	NM_001184.2	ataxia telangiectasia and Rad3 related	Checkpoint Activation - Cell Cycle and Signaling
ATRIP	NM_130384.1	ATR interacting protein	Checkpoint Activation
AURKA	NM_003600.2	aurora kinase A	Cell Cycle and Signaling
BCL2	NM_000657.2	B-cell CLL/lymphoma 2	Apoptosis
BCL2L1	NM_138578.1	BCL2-like 1	Apoptosis
BLM	NM_000057.2	Bloom syndrome, RecQ helicase-like	Homologous Recombination
BRCA1	NM_007305.2	breast cancer 1, early onset	Homologous Recombination
BRCA2	NM_000059.3	breast cancer 2, early onset	Homologous Recombination
BRIP1	NM_032043.1	BRCA1 interacting protein C-terminal helicase 1	Fanconi Anemia
BUB1B	NM_001211.4	BUB1 mitotic checkpoint serine/threonine kinase B	Cell Cycle and Signaling
CASP8	NM_001228.4	caspase 8, apoptosis-related cysteine peptidase	Apoptosis
CCND1	NM_053056.2	cyclin D1	Cell Cycle and Signaling
CCND2	NM_001759.2	cyclin D2	Cell Cycle and Signaling
CCND3	NM_001760.2	cyclin D3	Cell Cycle and Signaling

CCNO	NM_021147.3	cyclin O	Base Excision Repair
CDK7	NM_001799.2	cyclin-dependent kinase 7	Nucleotide Excision Repair - Cell Cycle and Signaling
CDKN1A	NM_000389.2	cyclin-dependent kinase inhibitor 1A (p21, Cip1)	Cell Cycle and Signaling
CDKN1B	NM_004064.2	cyclin-dependent kinase inhibitor 1B (p27, Kip1)	Cell Cycle and Signaling
CDKN2A	NM_000077.3	cyclin-dependent kinase inhibitor 2A	Cell Cycle and Signaling
CDKN2C	NM_001262.2	cyclin-dependent kinase inhibitor 2C (p18, inhibits CDK4)	Cell Cycle and Signaling
CHEK1	NM_001114121.1	checkpoint kinase 1	Checkpoint Activation - Cell Cycle and Signaling
CHEK2	NM_007194.3	checkpoint kinase 2	Checkpoint Activation - Cell Cycle and Signaling
CREBBP	NM_001079846.1	CREB binding protein	Cell Cycle and Signaling
CRY1	NM_004075.3	cryptochrome circadian clock 1	Independent Repair Enzymes/Polymerases
DDB1	NM_001923.3	damage-specific DNA binding protein 1, 127kDa	Nucleotide Excision Repair
DDB2	NM_000107.1	damage-specific DNA binding protein 2, 48kDa	Nucleotide Excision Repair
DNA2	NM_001080449.2	DNA replication helicase/nuclease 2	Independent Repair Enzymes/Polymerases
EGFR	NM_201282.1	epidermal growth factor receptor	Cell Cycle and Signaling
ERCC1	NM_001983.3	excision repair cross-complementing rodent repair deficiency, complementation group 1	Nucleotide Excision Repair
ERCC2	NM_000400.2	excision repair cross-complementing rodent repair deficiency, complementation group 2	Nucleotide Excision Repair
ERCC3	NM_000122.1	excision repair cross-complementing rodent repair deficiency, complementation group 3	Nucleotide Excision Repair
ERCC4	NM_005236.2	excision repair cross-complementing rodent repair deficiency, complementation group 4	Nucleotide Excision Repair
ERCC5	NM_000123.2	excision repair cross-complementing rodent repair deficiency, complementation group 5	Nucleotide Excision Repair
ERCC6	NM_000124.2	excision repair cross-complementing rodent repair deficiency, complementation group 6	Nucleotide Excision Repair

ERCC8	NM_000082.3	excision repair cross-complementing rodent repair deficiency, complementation group 8	Nucleotide Excision Repair
EXO1	NM_006027.3	exonuclease 1	Mismatch Repair
FAN1	NM_001146094.1	FANCD2/FANCI-associated nuclease 1	Fanconi Anemia
FANCA	NM_000135.2	Fanconi anemia, complementation group A	Fanconi Anemia
FANCB	NM_152633.2	Fanconi anemia, complementation group B	Fanconi Anemia
FANCC	NM_000136.2	Fanconi anemia, complementation group C	Fanconi Anemia
FANCD2	NM_033084.3	Fanconi anemia, complementation group D2	Fanconi Anemia
FANCE	NM_021922.2	Fanconi anemia, complementation group E	Fanconi Anemia
FANCF	NM_022725.2	Fanconi anemia, complementation group F	Fanconi Anemia
FANCG	NM_004629.1	Fanconi anemia, complementation group G	Fanconi Anemia
FANCI	NM_001113378.1	Fanconi anemia, complementation group I	Fanconi Anemia
FANCL	NM_001114636.1	Fanconi anemia, complementation group L	Fanconi Anemia
FANCM	NM_020937.2	Fanconi anemia, complementation group M	Fanconi Anemia
FEN1	NM_004111.4	flap structure-specific endonuclease 1	Base Excision Repair
GEN1	NM_182625.3	GEN1 Holliday junction 5' flap endonuclease	Homologous Recombination
GTF2H3	NM_001516.3	general transcription factor IIH, polypeptide 3, 34kDa	Nucleotide Excision Repair
H2AFX	NM_002105.2	H2A histone family, member X	Checkpoint Activation
HDAC1	NM_004964.2	histone deacetylase 1	Cell Cycle and Signaling
HDAC2	NM_001527.1	histone deacetylase 2	Cell Cycle and Signaling
HLTF	NM_139048.2	helicase-like transcription factor	Independent Repair Enzymes/Polymerases - Translesion Synthesis
HUS1	NM_004507.2	HUS1 checkpoint homolog (S. pombe)	Checkpoint Activation
KRAS	NM_004985.3	Kirsten rat sarcoma viral oncogene homolog	Cell Cycle and Signaling
LIG1	NM_000234.1	ligase I, DNA, ATP-dependent	Base Excision Repair
LIG3	NM_002311.3	ligase III, DNA, ATP-dependent	Base Excision Repair
LIG4	NM_002312.3	ligase IV, DNA, ATP-dependent	Non-homologous End Joining

MAD2L2	NM_001127325.1	MAD2 mitotic arrest deficient-like 2 (yeast)	Independent Repair Enzymes/Polymerases - Cell Cycle and Signaling
MDC1	NM_014641.2	mediator of DNA-damage checkpoint 1	Cell Cycle and Signaling
MGMT	NM_002412.3	O-6-methylguanine-DNA methyltransferase	Independent Repair Enzymes/Polymerases
MLH1	NM_000249.2	mutL homolog 1	Mismatch Repair
MLH3	NM_014381.2	mutL homolog 3	Mismatch Repair
MNAT1	NM_002431.2	MNAT CDK-activating kinase assembly factor 1	Nucleotide Excision Repair
MPG	NM_001015052.1	N-methylpurine-DNA glycosylase	Base Excision Repair
MRE11A	NM_005591.3	MRE11 meiotic recombination 11 homolog A (S. cerevisiae)	Homologous Recombination
MSH2	NM_000251.1	mutS homolog 2	Mismatch Repair
MSH3	NM_002439.2	mutS homolog 3	Mismatch Repair
MSH4	NM_002440.3	mutS homolog 4	Mismatch Repair
MSH5	NM_172165.2	mutS homolog 5	Mismatch Repair
MSH6	NM_000179.1	mutS homolog 6	Mismatch Repair
MUTYH	NM_012222.2	mutY homolog	Base Excision Repair
MYC	NM_002467.3	v-myc avian myelocytomatosis viral oncogene homolog	Cell Cycle and Signaling
MYD88	NM_002468.3	myeloid differentiation primary response 88	Apoptosis
NBN	NM_001024688.1	nibrin	Homologous Recombination
NEIL1	NM_024608.2	nei endonuclease VIII-like 1 (E. coli)	Base Excision Repair
NEIL2	NM_145043.2	nei endonuclease VIII-like 2 (E. coli)	Base Excision Repair
NEIL3	NM_018248.2	nei endonuclease VIII-like 3 (E. coli)	Base Excision Repair
NFKB1	NM_003998.2	nuclear factor of kappa light polypeptide gene enhancer in B-cells 1	Apoptosis
NKX3-1	NR_046072.1	NK3 homeobox 1	Cell Cycle and Signaling
NLRP2	NM_017852.1	NLR family, pyrin domain containing 2	Apoptosis
NTHL1	NM_002528.5	nth endonuclease III-like 1 (E. coli)	Base Excision Repair
OGG1	NM_002542.5	8-oxoguanine DNA glycosylase	Base Excision Repair
PARP1	NM_001618.3	poly (ADP-ribose) polymerase 1	Base Excision Repair
PARP2	NM_005484.3	poly (ADP-ribose) polymerase 2	Base Excision Repair
PARP3	NM_005485.4	poly (ADP-ribose) polymerase family, member 3	Base Excision Repair

PARP4	NM_006437.3	poly (ADP-ribose) polymerase family, member 4	Base Excision Repair
PCNA	NM_002592.2	proliferating cell nuclear antigen	Base Excision Repair - Translesion Synthesis - Cell Cycle and Signaling
PIK3CA	NM_006218.2	phosphatidylinositol-4,5-bisphosphate 3-kinase, catalytic subunit alpha	Apoptosis
PIK3CB	NM_006219.1	phosphatidylinositol-4,5-bisphosphate 3-kinase, catalytic subunit beta	Apoptosis
PIK3R1	NM_181504.2	phosphoinositide-3-kinase, regulatory subunit 1 (alpha)	Apoptosis
PMS1	NM_000534.4	PMS1 postmeiotic segregation increased 1 (S. cerevisiae)	Mismatch Repair
PMS2	NM_000535.5	PMS2 postmeiotic segregation increased 2 (S. cerevisiae)	Mismatch Repair
PNKP	NM_007254.2	polynucleotide kinase 3'-phosphatase	Base Excision Repair
POLB	NM_002690.1	polymerase (DNA directed), beta	Independent Repair Enzymes/Polymerases - Base Excision Repair
POLD1	NM_002691.2	polymerase (DNA directed), delta 1, catalytic subunit	Independent Repair Enzymes/Polymerases - Base Excision Repair
POLD3	NM_006591.2	polymerase (DNA-directed), delta 3, accessory subunit	Independent Repair Enzymes/Polymerases - Base Excision Repair
POLD4	NM_021173.2	polymerase (DNA-directed), delta 4, accessory subunit	Independent Repair Enzymes/Polymerases - Base Excision Repair
POLE	NM_006231.3	polymerase (DNA directed), epsilon, catalytic subunit	Independent Repair Enzymes/Polymerases
POLE2	NM_002692.2	polymerase (DNA directed), epsilon 2, accessory subunit	Independent Repair Enzymes/Polymerases - Base Excision Repair
POLE4	NM_019896.2	polymerase (DNA-directed), epsilon 4, accessory subunit	Independent Repair Enzymes/Polymerases
POLI	NM_007195.2	polymerase (DNA directed) iota	Independent Repair Enzymes/Polymerases - Translesion Synthesis
POLK	NM_016218.2	polymerase (DNA directed) kappa	Independent Repair Enzymes/Polymerases
POLL	NM_001174085.1	polymerase (DNA directed), lambda	Independent Repair Enzymes/Polymerases - Base Excision Repair
POLM	NM_013284.3	polymerase (DNA directed), mu	Independent Repair Enzymes/Polymerases

POLQ	NM_199420.3	polymerase (DNA directed), theta	Independent Repair Enzymes/Polymerases
POLR2D	NM_004805.3	polymerase (RNA) II (DNA directed) polypeptide D	Independent Repair Enzymes/Polymerases - Nucleotide Excision Repair
POLR2H	NM_001278698.1	polymerase (RNA) II (DNA directed) polypeptide H	Independent Repair Enzymes/Polymerases - Nucleotide Excision Repair
POLR2J	NM_006234.4	polymerase (RNA) II (DNA directed) polypeptide J, 13.3kDa	Independent Repair Enzymes/Polymerases - Nucleotide Excision Repair
PRKACB	NM_182948.2	protein kinase, cAMP-dependent, catalytic, beta	Apoptosis
PRKDC	NM_006904.6	protein kinase, DNA-activated, catalytic polypeptide	Non-homologous End Joining - Cell Cycle and Signaling
PRKX	NM_005044.1	protein kinase, X-linked	Apoptosis - Cell Cycle and Signaling
PTEN	NM_000314.4	phosphatase and tensin homolog	Nucleotide Excision Repair - Apoptosis
RAD1	NM_133377.2	RAD1 homolog (S. pombe)	Checkpoint Activation
RAD17	NM_133338.1	RAD17 homolog (S. pombe)	Checkpoint Activation
RAD18	NM_020165.2	RAD18 homolog (S. cerevisiae)	Translesion Synthesis
RAD21	NM_006265.2	RAD21 homolog (S. pombe)	Cell Cycle and Signaling
RAD23A	NM_005053.2	RAD23 homolog A (S. cerevisiae)	Nucleotide Excision Repair
RAD23B	NM_002874.3	RAD23 homolog B (S. cerevisiae)	Nucleotide Excision Repair
RAD50	NM_005732.2	RAD50 homolog (S. cerevisiae)	Homologous Recombination
RAD51	NM_133487.2	RAD51 recombinase	Homologous Recombination
RAD51B	NM_002877.5	RAD51 paralog B	Homologous Recombination
RAD51C	NM_002876.2	RAD51 paralog C	Homologous Recombination
RAD51D	NM_002878.3	RAD51 paralog D	Homologous Recombination
RAD52	NM_134424.2	RAD52 homolog (S. cerevisiae)	Homologous Recombination
RAD54L	NM_003579.2	RAD54-like (S. cerevisiae)	Homologous Recombination
RAD9A	NM_004584.2	RAD9 homolog A (S. pombe)	Checkpoint Activation
RB1	NM_000321.1	retinoblastoma 1	Cell Cycle and Signaling
RECQL	NM_032941.2	RecQ protein-like (DNA helicase Q1-like)	Homologous Recombination
RECQL5	NM_004259.6	RecQ protein-like 5	Homologous Recombination
REV1	NM_016316.2	REV1, polymerase (DNA directed)	Independent Repair Enzymes/Polymerases

RFC1	NM_001204747.1	replication factor C (activator 1) 1, 145kDa	Mismatch Repair - Translesion Synthesis
RFC3	NM_002915.3	replication factor C (activator 1) 3, 38kDa	Mismatch Repair - Translesion Synthesis
RFC4	NM_181573.2	replication factor C (activator 1) 4, 37kDa	Mismatch Repair - Translesion Synthesis
RMI1	NM_024945.2	RecQ mediated genome instability 1	Cell Cycle and Signaling
RMI2	NM_152308.1	RecQ mediated genome instability 2	Cell Cycle and Signaling
RPA1	NM_002945.3	replication protein A1, 70kDa	Nucleotide Excision Repair
RPA3	NM_002947.3	replication protein A3, 14kDa	Nucleotide Excision Repair
RPS27A	NM_002954.5	ribosomal protein S27a	Cell Cycle and Signaling
RRM2B	NM_015713.3	ribonucleotide reductase M2 B (TP53 inducible)	Independent Repair Enzymes/Polymerases - Cell Cycle and Signaling
SIRT1	NM_012238.4	sirtuin 1	Cell Cycle and Signaling
SLFN11	NM_001104587.1	schlafen family member 11	Apoptosis - Cell Cycle and Signaling
SLK	NM_014720.2	STE20-like kinase	Nucleotide Excision Repair
SLX4	NM_032444.2	SLX4 structure-specific endonuclease subunit	Homologous Recombination
SMAD4	NM_005359.3	SMAD family member 4	Cell Cycle and Signaling
SMARCA 4	NM_003072.3	SWI/SNF related, matrix associated, actin dependent regulator of chromatin, subfamily a, member 4	Cell Cycle and Signaling
SMC1A	NM_006306.2	structural maintenance of chromosomes 1A	Cell Cycle and Signaling
SMC3	NM_005445.3	structural maintenance of chromosomes 3	Cell Cycle and Signaling
SMUG1	NM_001243789.1	single-strand-selective monofunctional uracil-DNA glycosylase 1	Base Excision Repair
SUMO3	NM_006936.2	small ubiquitin-like modifier 3	Cell Cycle and Signaling
TDG	NM_003211.4	thymine-DNA glycosylase	Base Excision Repair
TIPIN	NM_017858.2	TIMELESS interacting protein	Checkpoint Activation
TOP3A	NM_004618.3	topoisomerase (DNA) III alpha	Homologous Recombination
TOP3B	NM_003935.4	topoisomerase (DNA) III beta	Homologous Recombination
TP53	NM_000546.2	tumor protein p53	Checkpoint Activation - Apoptosis - Cell Cycle and Signaling
TP53BP1	NM_001141980.1	tumor protein p53 binding protein 1	Apoptosis
TREX1	NM_016381.3	three prime repair exonuclease 1	Independent Repair Enzymes/Polymerases

UBB	NM_018955.2	ubiquitin B	Cell Cycle and Signaling
UBE2T	NM_014176.3	ubiquitin-conjugating enzyme E2T (putative)	Fanconi Anemia
UNG	NM_003362.3	uracil-DNA glycosylase	Base Excision Repair
USP1	NM_003368.4	ubiquitin specific peptidase 1	Fanconi Anemia
WEE1	NM_003390.3	WEE1 G2 checkpoint kinase	Cell Cycle and Signaling
WRN	NM_000553.4	Werner syndrome, RecQ helicase-like	Homologous Recombination
XPA	NM_000380.3	xeroderma pigmentosum, complementation group A	Nucleotide Excision Repair
XPC	NM_004628.3	xeroderma pigmentosum, complementation group C	Nucleotide Excision Repair
XRCC1	NM_006297.2	X-ray repair complementing defective repair in Chinese hamster cells 1	Base Excision Repair
XRCC2	NM_005431.1	X-ray repair complementing defective repair in Chinese hamster cells 2	Homologous Recombination
XRCC3	NM_001100119.1	X-ray repair complementing defective repair in Chinese hamster cells 3	Homologous Recombination
XRCC4	NM_003401.3	X-ray repair complementing defective repair in Chinese hamster cells 4	Non-homologous End Joining
XRCC5	NM_021141.3	X-ray repair complementing defective repair in Chinese hamster cells 5 (double-strand-break rejoining)	Non-homologous End Joining
XRCC6	NM_001469.3	X-ray repair complementing defective repair in Chinese hamster cells 6	Non-homologous End Joining
Internal Reference Genes			
CC2D1B	NM_032449.2	coiled-coil and C2 domain containing 1B	
COG7	NM_153603.3	component of oligomeric golgi complex 7	
EDC3	NM_001142443.1	enhancer of mRNA decapping 3	
GPATCH3	NM_022078.2	G patch domain containing 3	
HDAC3	NM_003883.2	histone deacetylase 3	
MTMR14	NM_022485.3	myotubularin related protein 14	
NUBP1	NM_001278506.1	nucleotide binding protein 1	
PRPF38A	NM_032864.3	pre-mRNA processing factor 38A	
SAP130	NM_024545.3	Sin3A-associated protein, 130kDa	
SF3A3	NM_006802.2	splicing factor 3a, subunit 3, 60kDa	
TLK2	NM_006852.2	tousled-like kinase 2	
ZC3H14	NM_001160103.1	zinc finger CCCH-type containing 14	

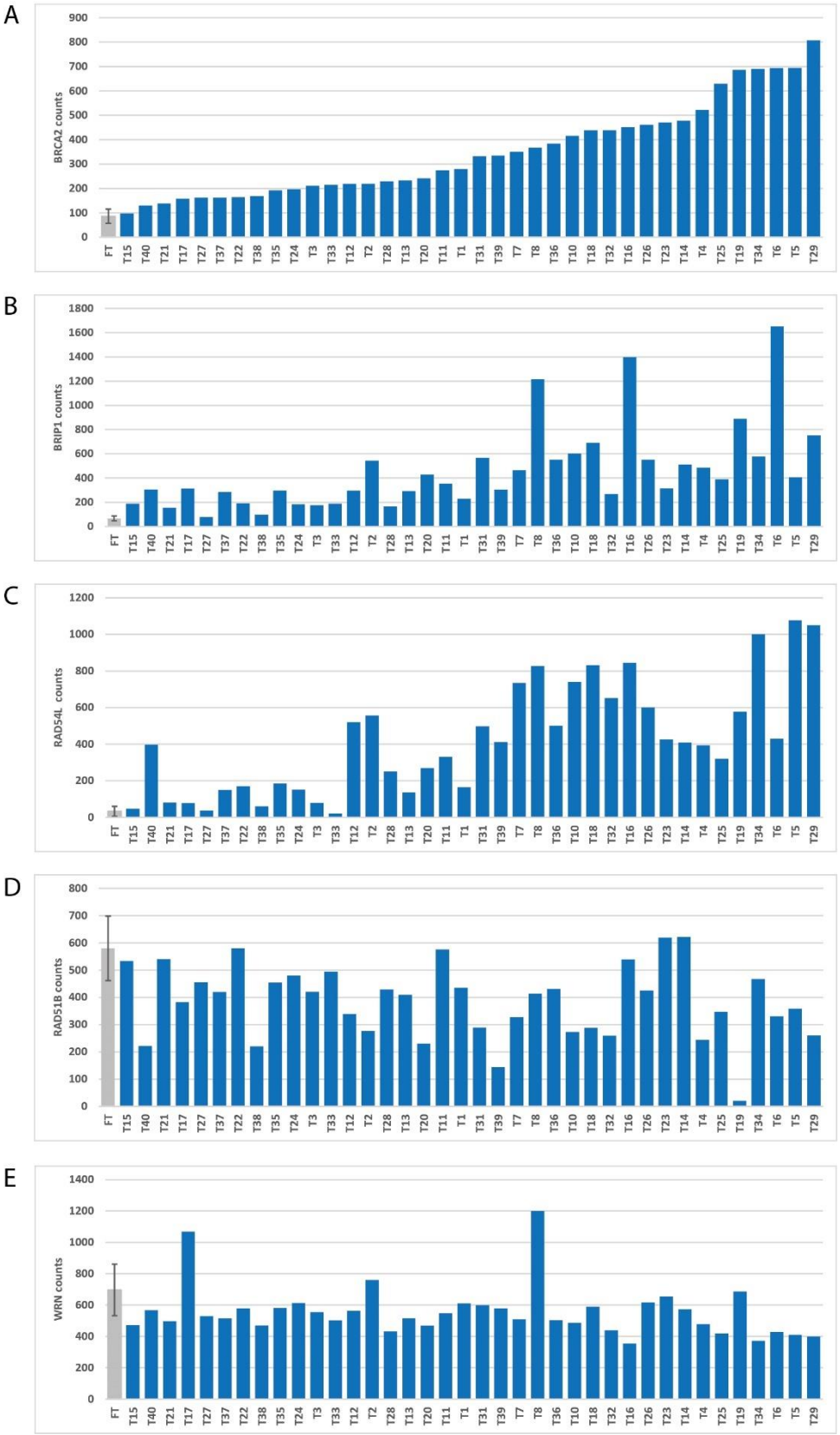

Supplementary Figure 1: Expression values (mRNA counts) obtained with the NanoString nCounter assay for the indicated Homologous Recombination and Fanconi Anemia genes. For the 11 normal fallopian tube (FT) samples, the mean and standard deviation are depicted. Individual values for each of the 38 tumors (T) are shown. Tumor samples have been ordered from lowest to highest BRCA2 expression level.

References

Alsop, K., Fereday, S., Meldrum, C., DeFazio, A., Emmanuel, C., George, J., Dobrovic, A., Birrer, M. J., Webb, P. M., Stewart, C., Friedlander, M., Fox, S., Bowtell, D., & Mitchell, G. (2012). BRCA mutation frequency and patterns of treatment response in BRCA mutation-positive women with ovarian cancer: A report from the Australian ovarian cancer study group. *Journal of Clinical Oncology*, *30*(33), 2654–2663. https://doi.org/10.1200/JCO.2011.39.8545

American Cancer Society. (2021). *Cancer Facts & Figures 202American Cancer Society. (2021). Cancer Facts & Figures 2021. https://www.cancer.org/content/dam/cancer-org/research/cancer-facts-and-statistics/annual-cancer-facts-and-figures/2021/cancer-facts-and-figures-2021.pdf1*. https://www.cancer.org/content/dam/cancer-org/research/cancer-facts-and-statistics/annual-cancer-facts-and-figures/2021/cancer-facts-and-figures-2021.pdf

Baldwin, R. L., Nemeth, E., Tran, H., Shvartsman, H., Cass, I., Narod, S., & Karlan, B. Y. (2000). BRCA1 promoter region hypermethylation in ovarian carcinoma: A population-based study. *Cancer Research*, *60*(19), 5329–5333.

Bowtell, D. D., Böhm, S., Ahmed, A. A., Aspuria, P., Jr, C. B., Beral, V., Berek, J. S., Birrer, M. J., Blagden, S., Bookman, M. A., Brenton, J. D., Chiappinelli, K. B., Correia, F., Coukos, G., Drapkin, R., Edmondson, R., Gabra, H., Galon, J., Gourley, C., … Balkwill, F. R. (2015). Rethinking ovarian cancer II: reducing mortality from high-grade serous ovarian cancer. *Nature Reviews Cancer*, *15*(11), 668–679. https://doi.org/10.1038/nrc4019

Brown, J. S., O'Carrigan, B., Jackson, S. P., & Yap, T. A. (2017). Targeting DNA repair in cancer: Beyond PARP inhibitors. *Cancer Discovery*, *7*(1), 20–37. https://doi.org/10.1158/2159-8290.CD-16-0860

Carser, J. E., Quinn, J. E., Michie, C. O., O'Brien, E. J., McCluggage, W. G., Maxwell, P., Lamers, E., Lioe, T. F., Williams, A. R. W., Kennedy, R. D., Gourley, C., & Harkin, D. P. (2011). BRCA1 is both a prognostic and predictive biomarker of response to chemotherapy in sporadic epithelial ovarian cancer. *Gynecologic Oncology*, *123*(3), 492–498. https://doi.org/10.1016/j.ygyno.2011.08.017

Chang, Y. F., Imam, J. S., & Wilkinson, M. F. (2007). The Nonsense-mediated decay RNA surveillance pathway. *Annual Review of Biochemistry*, *76*, 51–74. https://doi.org/10.1146/annurev.biochem.76.050106.093909

Cortez, A. J., Tudrej, P., Kujawa, K. A., & Lisowska, K. M. (2018). Advances in ovarian cancer therapy. *Cancer Chemotherapy and Pharmacology*, *81*(1), 17–38. https://doi.org/10.1007/s00280-017-3501-8

Esteller, M., Silva, J. M., Dominguez, G., Bonilla, F., Matias-Guiu, X., Lerma, E., Bussaglia, E., Prat, J., Harkes, I. C., Repasky, E. A., Gabrielson, E., Schutte, M., Baylin, S. B., & Herman, J. G. (2000). Promoter hypermethylation and BRCA1 inactivation in sporadic breast and ovarian tumors. *Journal of the National Cancer Institute*, *92*(7), 564–569. https://doi.org/10.1093/jnci/92.7.564

Fong, P. C., Yap, T. A., Boss, D. S., Carden, C. P., Mergui-Roelvink, M., Gourley, C., De Greve, J., Lubinski, J., Shanley, S., Messiou, C., A'Hern, R., Tutt, A., Ashworth, A., Stone, J., Carmichael, J., Schellens, J. H. M., De Bono, J. S., & Kaye, S. B. (2010). Poly(ADP)-ribose polymerase inhibition: Frequent durable responses in BRCA carrier ovarian cancer correlating with platinum-free interval. *Journal of Clinical Oncology*, *28*(15), 2512–2519. https://doi.org/10.1200/JCO.2009.26.9589

Gao, Y., Zhu, J., Zhang, X., Wu, Q., Jiang, S., Liu, Y., Hu, Z., Liu, B., & Chen, X. (2013). BRCA1 mRNA Expression as a Predictive and Prognostic Marker in Advanced Esophageal Squamous Cell Carcinoma Treated with Cisplatin- or Docetaxel-Based Chemotherapy/Chemoradiotherapy. *PLoS ONE*, *8*(1). https://doi.org/10.1371/journal.pone.0052589

Gee, M. E., Faraahi, Z., McCormick, A., & Edmondson, R. J. (2018). DNA damage repair in ovarian cancer: Unlocking the heterogeneity. *Journal of Ovarian Research*, *11*(50), 1–12. https://doi.org/10.1186/s13048-018-0424-x

Geiss, G. K., Bumgarner, R. E., Birditt, B., Dahl, T., Dowidar, N., Dunaway, D. L., Fell, H. P., Ferree, S., George, R. D., Grogan, T., James, J. J., Maysuria, M., Mitton, J. D., Oliveri, P., Osborn, J. L., Peng, T., Ratcliffe, A. L., Webster, P. J., Davidson, E. H., … Dimitrov, K. (2008). Direct multiplexed measurement of gene expression with color-coded probe pairs. *Nature Biotechnology*, *26*(3), 317–326. https://doi.org/10.1038/nbt1385

Hu, Z., Artibani, M., Alsaadi, A., Wietek, N., Morotti, M., Shi, T., Zhong, Z., Santana Gonzalez, L., El-Sahhar, S., KaramiNejadRanjbar, M., Mallett, G., Feng, Y., Masuda, K., Zheng, Y., Chong, K., Damato, S., Dhar, S., Campo, L., Garruto Campanile, R., … Ahmed, A. A. (2020). The Repertoire of Serous Ovarian Cancer Non-genetic Heterogeneity Revealed by Single-Cell Sequencing of Normal Fallopian Tube Epithelial Cells. *Cancer Cell*, *37*(2), 226-242.e7. https://doi.org/10.1016/j.ccell.2020.01.003

Hu, Z., Yau, C., & Ahmed, A. A. (2017). A pan-cancer genome-wide analysis reveals tumour dependencies by induction of nonsense-mediated decay. *Nature Communications*, *8*, 1–9. https://doi.org/10.1038/ncomms15943

Huang, Y., Wu, P., Liu, B., & Du, J. (2016). Successful personalized chemotherapy for metastatic gastric cancer based on quantitative BRCA1 mRNA expression level: A case report. *Oncology Letters*, *11*(6), 4183–4186. https://doi.org/10.3892/ol.2016.4546

Kuchenbaecker, K. B., Hopper, J. L., Barnes, D. R., Phillips, K. A., Mooij, T. M., Roos-Blom, M. J., Jervis, S., Van Leeuwen, F. E., Milne, R. L., Andrieu, N., Goldgar, D. E., Terry, M. B., Rookus, M. A., Easton, D. F., & Antoniou, A. C. (2017). Risks of breast, ovarian, and contralateral breast cancer for BRCA1 and BRCA2 mutation carriers. *JAMA - Journal of the American Medical Association*, *317*(23), 2402–2416. https://doi.org/10.1001/jama.2017.7112

Labidi-Galy, S. I., Papp, E., Hallberg, D., Niknafs, N., Adleff, V., Noe, M., Bhattacharya, R., Novak, M., Jones, S., Phallen, J., Hruban, C. A., Hirsch, M. S., Lin, D. I., Schwartz, L., Maire, C. L., Tille, J. C., Bowden, M., Ayhan, A., Wood, L. D., … Velculescu, V. E. (2017). High grade serous ovarian carcinomas originate in the fallopian tube. *Nature Communications*, *8*, 1–11. https://doi.org/10.1038/s41467-017-00962-1

Lheureux, S., Gourley, C., Vergote, I., & Oza, A. M. (2019). Epithelial ovarian cancer. *The Lancet*, *393*, 1240–1253. https://doi.org/10.1016/S0140-6736(18)32552-2

Lindeboom, R. G. H., Supek, F., & Lehner, B. (2016). The rules and impact of nonsense-mediated mRNA decay in human cancers. *Nature Genetics*, *48*(10), 1112–1118. https://doi.org/10.1038/ng.3664.The

Lisio, M. A., Fu, L., Goyeneche, A., Gao, Z. H., & Telleria, C. (2019). High-grade serous ovarian cancer: Basic sciences, clinical and therapeutic standpoints. *International Journal of Molecular Sciences*, *20*(4), 952. https://doi.org/10.3390/ijms20040952

Lord, C. J., & Ashworth, A. (2012). The DNA damage response and cancer therapy. *Nature*, *481*(7381), 287–294. https://doi.org/10.1038/nature10760

Machado, P. M., Brandão, R. D., Cavaco, B. M., Eugénio, J., Bento, S., Nave, M., Rodrigues, P., Fernandes, A., & Vaz, F. (2007). Screening for a BRCA2 rearrangement in high-risk breast/ovarian cancer families: Evidence for a founder effect and analysis of the associated phenotypes. *Journal of Clinical Oncology*, *25*(15), 2027–2034. https://doi.org/10.1200/JCO.2006.06.9443

Mateo, J., Lord, C. J., Serra, V., Tutt, A., Balmaña, J., Castroviejo-Bermejo, M., Cruz, C., Oaknin, A., Kaye, S. B., & De Bono, J. S. (2019). A decade of clinical development of PARP inhibitors in perspective. *Annals of Oncology*, *30*(9), 1437–1447. https://doi.org/10.1093/annonc/mdz192

Matulonis, U. A., Sood, A. K., Fallowfield, L., Howitt, B. E., Sehouli, J., & Karlan, B. Y. (2016). Ovarian cancer. *Nature Reviews Disease Primers*, *2*, 1–22. https://doi.org/10.1038/nrdp.2016.61

Metcalfe, K. A., Poll, A., Royer, R., Llacuachaqui, M., Tulman, A., Sun, P., & Narod, S. A. (2010). Screening for founder mutations in BRCA1 and BRCA2 in unselected Jewish women. *Journal of Clinical Oncology*, *28*(3), 387–391. https://doi.org/10.1200/JCO.2009.25.0712

Moskwa, P., Buffa, F. M., Pan, Y., Panchakshari, R., Muschel, R. J., Beech, J., Kulshrestha, R., Abdelmohsen, K., Weinstock, M., Gorospe, M., Harris, A. L., & Helleday, T. (2011). miR-182-mediated down-regulation of BRCA1 impacts DNA repair and sensitivity to PARP inhibitors. *Molecular Cell*, *41*(2), 210–220. https://doi.org/10.1016/j.molcel.2010.12.005.miR-182-mediated

Network, C. G. A. R. (2011). Integrated genomic analyses of ovarian carcinoma. *Nature*, *474*(7353), 609–615. https://doi.org/10.1038/nature10166

North, B. V., Curtis, D., & Sham, P. C. (2003). A Note on the Calculation of Empirical P Values from Monte Carlo Procedures. *The American Journal of Human Genetics*, *72*, 498–499. https://doi.org/10.1086/367548

Patel, P. G., Selvarajah, S., Guérard, K. P., Bartlett, J. M. S., Lapointe, J., Berman, D. M., Okello, J. B. A., & Park, P. C. (2017). Reliability and performance of commercial RNA and DNA extraction kits for FFPE tissue cores. *PLoS ONE*, *12*(6), 1–16. https://doi.org/10.1371/journal.pone.0179732

Peixoto, A., Santos, C., Pinto, P., Pinheiro, M., & Rocha, P. (2015). Screening for a BRCA2

Rearrangement in High-Risk Breast/ Ovarian Cancer Families: Evidence for a Founder Effect and Analysis of the Associated Phenotypes. *Clinical Genetics*, *88*, 41–48.

Peng, G., Lin, C. C. J., Mo, W., Dai, H., Park, Y. Y., Kim, S. M., Peng, Y., Mo, Q., Siwko, S., Hu, R., Lee, J. S., Hennessy, B., Hanash, S., Mills, G. B., & Lin, S. Y. (2014). Genome-wide transcriptome profiling of homologous recombination DNA repair. *Nature Communications*, *5*, 1–11. https://doi.org/10.1038/ncomms4361

Pilié, P. G., Tang, C., Mills, G. B., & Yap, T. A. (2019). State-of-the-art strategies for targeting the DNA damage response in cancer. *Nature Reviews Clinical Oncology*, *16*(2), 81–104. https://doi.org/10.1038/s41571-018-0114-z

Prakash, R., Zhang, Y., Feng, W., & Jasin, M. (2015). Homologous recombination and human health: The roles of BRCA1, BRCA2, and associated proteins. *Cold Spring Harbor Perspectives in Biology*, *7*(4), 1–27. https://doi.org/10.1101/cshperspect.a016600

Quinn, J. E., James, C. R., Stewart, G. E., Mulligan, J. M., White, P., Chang, G. K. F., Mullan, P. B., Johnston, P. G., Wilson, R. H., & Harkin, D. P. (2007). BRCA1 mRNA expression levels predict for overall survival in ovarian cancer after chemotherapy. *Clinical Cancer Research*, *13*(24), 7413–7420. https://doi.org/10.1158/1078-0432.CCR-07-1083

Rajan, J. V, Marquis, S. T., Gardner, H. P., & Chodosh, L. A. (1997). *Developmental Expression of Brca2 Colocalizes with Brca1 and Is Associated with Proliferation and Differentiation in Multiple Tissues*. *184*, 385–401.

Reis, P. P., Waldron, L., Goswami, R. S., Xu, W., Xuan, Y., Perez-Ordonez, B., Gullane, P., Irish, J., Jurisica, I., & Kamel-Reid, S. (2011). mRNA transcript quantification in archival samples using multiplexed, color-coded probes. *BMC Biotechnology*, *11*. https://doi.org/10.1186/1472-6750-11-46

Rosell, R., Perez-Roca, L., Sanchez, J. J., Cobo, M., Moran, T., Chaib, I., Provencio, M., Domine, M., Sala, M. A., Jimenez, U., Diz, P., Barneto, I., Macias, J. A., de las Peñas, R., Catot, S., Isla, D., Sanchez, J. M., Ibeas, R., Lopez-Vivanco, G., … Taron, M. (2009). Customized Treatment in Non-Small-Cell Lung Cancer Based on EGFR Mutations and BRCA1 mRNA Expression. *PLoS ONE*, *4*(5). https://doi.org/10.1371/journal.pone.0005133

Sung, H., Ferlay, J., Siegel, R. L., Laversanne, M., Soerjomataram, I., Jemal, A., & Bray, F. (2021). Global Cancer Statistics 2020: GLOBOCAN Estimates of Incidence and Mortality Worldwide for 36 Cancers in 185 Countries. *CA: A Cancer Journal for Clinicians*, *0*, 1–41. https://doi.org/10.3322/caac.21660

Swisher, E. M., Sakai, W., Karlan, B. Y., Wurz, K., Urban, N., & Taniguchi, T. (2008). *Secondary BRCA1 Mutations in BRCA1 -Mutated Ovarian Carcinomas with Platinum Resistance*. *8*, 2581–2587. https://doi.org/10.1158/0008-5472.CAN-08-0088

Taron, M., Rosell, R., Felip, E., Mendez, P., Souglakos, J., Ronco, M. S., Queralt, C., Majo, J., Sanchez, J. M., Sanchez, J. J., & Maestre, J. (2004). BRCA1 mRNA expression levels as an indicator of chemoresistance in lung cancer. *Human Molecular Genetics*, *13*(20), 2443–2449. https://doi.org/10.1093/hmg/ddh260

Tomasova, K., Cumova, A., Seborova, K., Horak, J., Koucka, K., Vodickova, L., Vaclavikova,

R., & Vodicka, P. (2020). DNA repair and ovarian carcinogenesis: Impact on risk, prognosis and therapy outcome. *Cancers*, *12*(7), 1–37. https://doi.org/10.3390/cancers12071713

Torre, L. A., Trabert, B., DeSantis, C. E., Miller, K. D., Samimi, G., Runowicz, C. D., Gaudet, M. M., Jemal, A., & Siegel, R. L. (2018). Ovarian cancer statistics, 2018. *CA: A Cancer Journal for Clinicians*, *68*(4), 284–296. https://doi.org/10.3322/caac.21456

Tsibulak, I., Wieser, V., Degasper, C., Shivalingaiah, G., Wenzel, S., Sprung, S., Lax, S. F., Marth, C., Fiegl, H., & Zeimet, A. G. (2018). BRCA1 and BRCA2 mRNA-expression prove to be of clinical impact in ovarian cancer. *British Journal of Cancer*, *119*(6), 683–692. https://doi.org/10.1038/s41416-018-0217-4

Tsibulak, I., Wieser, V., Welponer, H., Leitner, K., Hackl, H., Marth, C., Fiegl, H., & Zeimet, A. G. (2020). Clinical impact of BRCA2 mRNA expression in high-grade serous ovarian cancer: validation using the TCGA cohort. *Acta Oncologica*, *0*(0), 1–4. https://doi.org/10.1080/0284186X.2020.1841288

Vaz-Drago, R., Custódio, N., & Carmo-Fonseca, M. (2017). Deep intronic mutations and human disease. *Human Genetics*, *136*(9), 1093–1111. https://doi.org/10.1007/s00439-017-1809-4

Wang, L., Wei, J., Qian, X., Yin, H., Zhao, Y., Yu, L., Wang, T., & Liu, B. (2008). ERCC1 and BRCA1 mRNA expression levels in metastatic malignant effusions is associated with chemosensitivity to cisplatin and/or docetaxel. *BMC Cancer*, *8*(97), 1–7. https://doi.org/10.1186/1471-2407-8-97

Webb, P. M., & Jordan, S. J. (2017). Epidemiology of epithelial ovarian cancer. *Best Practice and Research: Clinical Obstetrics and Gynaecology*, *41*, 3–14. https://doi.org/10.1016/j.bpobgyn.2016.08.006

Acknowledgements

Gostaria de começar por agradecer à Professora Noélia por toda a ajuda incondicional ao longo destes anos, desde o meu início neste projeto. Um grande obrigado também à Rosina pela análise estatística e por me ter explicado os fundamentos básicos da mesma. Não podia de deixar de agradecer à Professora Carmo por me ter aceitado e por desde o 1º ano incitar os seus alunos a questionar as coisas e a ter espírito crítico. Agradeço, ainda, a todas as pessoas que intervieram de forma mais direta ou indireta ao longo deste trabalho.

Obrigada a toda a minha família pelo apoio ao longo destes 6 anos, que nem sempre foram fáceis (mas que grande eufemismo!). Em particular, destaco o apoio dos meus pais, do meu irmão David e dos meus avós Rosário, Higino, Zélia e João, que acompanharam mais de perto o meu percurso.

Finalmente, quero agradecer a todos os meus amigos da faculdade e de fora dela que tornaram esta jornada mais fácil e exequível. Eles sabem que são. Também estou profundamente grata ao Gonçalo por todo o seu apoio.